Korean J. Chem. Eng., 32(5), 852-859 (2015)
DOI: 10.1007/s11814-014-0270-5

pISSN: 0256-1115
eISSN: 1975-7220

Mesoporous silica with monodispersed pores synthesized from the controlled self-assembly of silica nanoparticles

Min Su*,, Hongjiu Su*,†, Baolei Du*,**, Xiaotong Li*,**, Gaoyuan Ren*, and Shudong Wang*,†**

*Dalian National Laboratory for Clean Energy, Dalian Institute of Chemical Physics, Chinese Academy of Sciences, Dalian 116023, Liaoning, China
**University of Chinese Academy of Sciences, Beijing 100049, China
(*Received 18 April 2014 • accepted 11 September 2014*)

Abstract−Silica nanoparticles with different sizes (ranging from 10 nm to 104 nm) and size distributions were synthesized by semi-batch and semi-batch/batch methods of the Stöber process. Then the amorphous silica with different surface areas (ranging from 30 m^2/g to 400 m^2/g) and pores (ranging from 3 nm to 33 nm) were obtained by various aging treatments and drying methods of the synthesized colloidal silica sol. The aging treatment resulted in the monodispersed pore distribution and decreased BET surface area of silica. The high-humidity drying method led to the mesoporous silica with uniform pores and decreased small pores. As the silica was obtained by the arrangement of silica nanoparticles, the pore diameter and pore distribution of mesoporous silica were directly related to the size and distribution of nanoparticles. Furthermore, this study offered a new thought for the synthesis of other mesoporous materials with uniform pore distributions.

Keywords: Mesoporous Silica, Silica Nanoparticles, Semi-batch/Batch, Semi-batch, Self-assembly

INTRODUCTION

Mesoporous silica, the material with high surface area and the pore size in the range of 2-50 nm, has attracted much attention for numerous applications in adsorption [1], catalysis [2] and drug delivery [3]. There are several methods used for the preparation of mesoporous silica. The most popular one, the sol-gel synthesis proposed by Stöber et al. [4], is based on hydrolysis and condensation of silicon-alkoxide precursor. In this method, the pore diameter, surface area and pore volume of mesoporous silica are directly related to the size and monodispersity of colloidal silica particles [5]. However, the silica particles obtained by this method generally possess poor monodispersity and irregular shapes [6,7].

Typically, the batch process used for the preparation of silica particles is simple and has the advantage of high conversions. However, the nanoparticles with narrow size distributions are not easily gained through the batch process. On the contrary, the semi-batch process [8] has greater controllability over the resulting particle size, shape and size distribution. This is due to the short nucleation time and the slow hydrolysis rate of the reaction obtained in the semi-batch process. Combining the advantages of batch and semi-batch processes, Kim et al. [9] obtained a narrower size distribution by the method of the semi-batch/batch than that by any single batch or semi-batch method. However, the pore size and specific area of mesoporous silica obtained from the two methods were seldom reported.

In the colloidal solution of silica, the silica particles are stably dispersed in the homogeneous solution without precipitation. And the arrangement of silica particles into packed structures is simply achieved by solvent evaporation [5,10,11]. The self-assembly by solvent evaporation is based on the attractive capillary forces operative during the solvent evaporation process. This route for producing mesoporous materials has been designated as the "hard-sphere packing" mechanism [12]. Because the mesoporous silica is obtained by the arrangement of silica nanoparticles, the pore in silica is just the void among particles. And the silica is amorphous. Furthermore, these packed materials can serve as the templates for fabricating other materials [13,14]. However, there is no report concerning how to obtain the mesoporous silica with monodispersed pores from silica nanoparticles.

We report here the syntheses of silica nanoparticles by using semi-batch (S) and mixed semi-batch/batch (S/B) methods of Stöber process. The silica nanoparticles with different sizes were obtained by varying the concentration of ammonia. Since the pore size of silica was greatly affected by the aging process, the colloidal solution was aged before the drying process. Unlike almost all the previous literatures [5,9,15,16], the colloidal sol in this experiment was directly dried without any separation. Then the mesoporous silica was obtained by the self-assembly of silica nanoparticles in the drying process. The drying procedure and aging process were both investigated to obtain the mesoporous silica with monodispersed pores.

EXPERIMENTAL

1. Chemicals

Tetraethyl orthosilicate (TEOS, kermel, Tianjin), ammonium hydroxide (25-28 wt%, kermel, Tianjin), ethanol (kermel, Tianjin) and all other reagents were used as received, without further puri-

†To whom correspondence should be addressed.
E-mail: wangsd@dicp.ac.cn, suhj@dicp.ac.cn

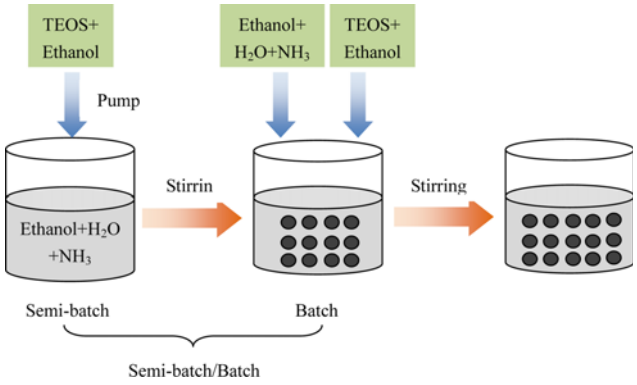

Fig. 1. Schematic drawing of the two methods (S and S/B) for preparing silica nanoparticles.

fication.

2. Synthesis of Silica Nanoparticles

Silica nanoparticles were synthesized via the hydrolysis of TEOS using two methods, S and S/B [9] processes. As for the S method, the solution A (a mixture of TEOS and ethanol) was fed into the reactor (volume=2 L) containing the solution B (a mixture of ammonia, water and ethanol) by a micro pump (LabAlliance Series || Pump) with a constant flow rate (5 ml/min). Then the solution was agitated for two hours at 80 °C. On the other hand, the method for the S/B process was as follows: after the S process (one hour of agitation, reactor volume=2 L), solutions A and B were again fed into the reactor simultaneously, and then the mixture of two solutions was vigorously stirred for another one hour. Note that the overall reaction time and reaction volume of the S/B process were the same as that of the S process. The overall experimental procedure and the schematic drawings of the two methods are shown in Fig. 1. The sample obtained from the S/B method at ammonia concentration of 0.1 mol/L was denoted as S/B-0.1M.

3. Synthesis of Mesoporous Silica Via Silica Nanoparticles

Once the silica nanoparticles were synthesized, they were aged in the sealed beaker at 25 °C for 0 hours, 24 hours and 48 hours, respectively. Thereafter, the aged colloidal sol (200 ml) was placed in the 500 ml beaker (diameter of 90 mm, height of 122 mm), and dried at 70 °C in oven with the relative humidity (RH) of 5% and 90%, respectively. For the colloidal silica sol completely dried at 70 °C and 5%, RH needed less than 6 hours, so samples were denoted as 0 h-5%RH, 24 h-5%RH and 48 h-5%RH, respectively. On the other hand, the colloidal silica sol completely dried at 90% RH needed 24 hours, so samples were expressed as 24 h-90%RH, 48 h-90%RH and 72 h-90%RH, respectively. Finally, all the obtained mesoporous silica was calcined at 500 °C for 4 hours.

4. Characterization

A Malvern Zetasizer Nano ZS90 was used to determine the mean particle size and size distribution of silica nanoparticles. Polydispersity index (PDI) was automatically calculated by the system software from the cumulant analysis as defined in ISO 13321:1996. Nitrogen adsorption/desorption isotherms of the mesoporous silica were taken by the Quantachrome NOVA 2200e. Pore size distribution curves were obtained from the desorption branch by using the Barrett-Joyner-Halenda (BJH) method. The surface area was calculated by the Brunauer-Emmett-Teller (BET) method. The transmission electron microscopy (TEM) measurement was carried out with a FEI Tecnai G2 Spirit equipment operated at an accelerating voltage of 120 kV. The reduced catalyst powder was ultrasonically dispersed in ethanol and dropped onto a copper grid with amorphous carbon film, then dried in air.

RESULTS AND DISCUSSION

1. The Effect of Ammonia Concentration on the Size and PDI of Silica Nanoparticles.

Fig. 2 presents the effect of ammonia concentration on the mean size and PDI of silica nanoparticles synthesized via the Stöber process. The average particle sizes of silica obtained from both the S/B and S methods increased with the ammonia concentration increasing. In addition, the mean size of silica particles synthesized from the S method was larger than that of the S/B method at the ammonia concentration from 0.1 mol/L to 0.8 mol/L. The PDI value represents the monodispersity of the silica particles. As the ammonia concentration increased from 0.1 mol/L to 0.8 mol/L, the PDI value of both S/B and S methods first decreased and then increased. Above all, this trend of particle size and size distribution agreed with the results of Kim et al. [9].

LaMer and Dinegar [17] proposed that the nucleation occurred over a finite period of time, and then the growth of particles would occur through a self-sharpening mechanism. The nucleation oc-

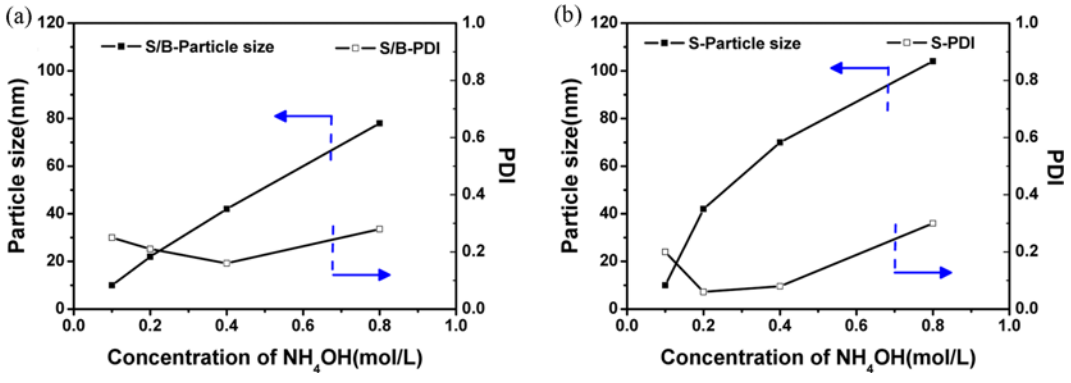

Fig. 2. The effect of ammonia concentration on the mean size and PDI of silica nanoparticles. (a) S/B method; (b) S method.

curred once the concentration of monomers reached a minimum critical supersaturation. Then, the particle growth and continuous nucleation [18] proceeded until the reaction stopped due to the equilibrium solubility. In the S system, the accumulation rate of growth units to a minimum critical supersaturation was slower than that of a batch system [9]. However, the growth time of particles in the batch system was shorter than that of S system, because TEOS and ammonia were fed into the reactor instantaneously. Therefore, the mean particle size of the S/B method was smaller than that of the S method. Matsoukas and Gulari [19] reported that the ammonia promoted the hydrolysis and polymerization rate simultaneously, resulting in faster kinetics and lager particle sizes. However, the silica depolymerization reaction took place at the high pH [20]. At high concentrations, the sample might contain two distinctly different particle sizes, which was in agreement with the research of Stöber [4].

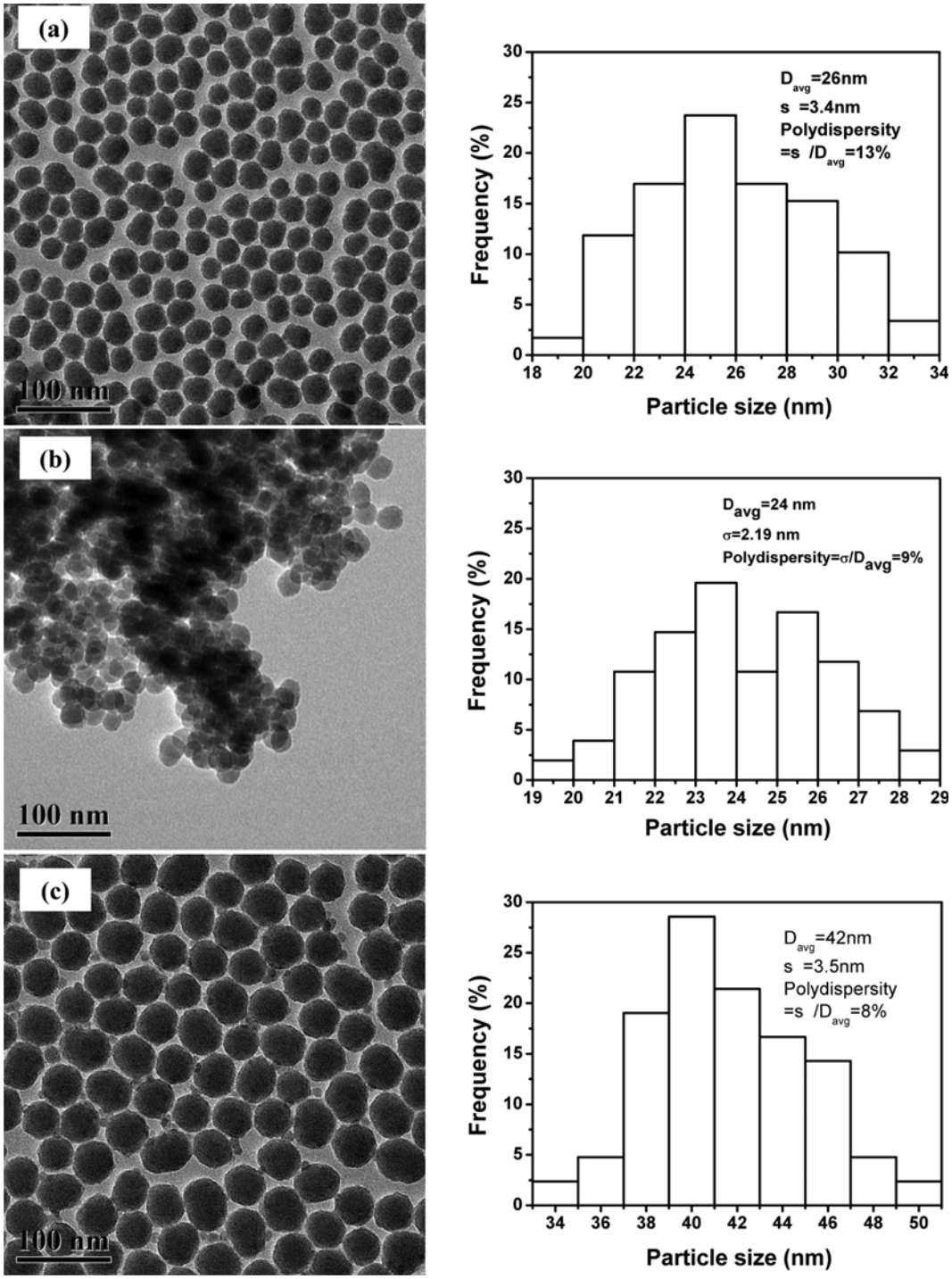

Fig. 3. TEM images of colloidal silica sol and the dried mesoporous silica: (a) S/B-0.2M; (b) S/B-0.2M-0h-5%RH; (c) S-0.2M.

The dynamic light scattering (DLS) results (Fig. 2) were confirmed by the TEM images (Fig. 3). As depicted in Fig. 3(a), 3(b) and 3(c), the size and PDI of silica particles were close to those of DLS results. The TEM image of mesoporous silica obtained from the drying of colloidal sol was shown in Fig. 3(b), which proved that the mesoporous silica was achieved by the random arrangement of nanoparticles. Beside, the particle size of mesoporous silica obtained from the drying process was a little smaller than that of the colloidal sol.

2. The Effect of Aging Time on the BET Surface Area of Mesoporous Silica Synthesized from the Self-assembly of Silica Nanoparticles

Table 1 presents the BET surface area of the mesoporous silica, which was synthesized from the colloidal silica sol after aging treatment. As shown in Table 1, the BET surface area of the mesoporous silica obtained from both S and S/B methods decreased with the ammonia concentration increasing. Both results are in a good agreement with the results of DLS. Because the mesoporous silica was obtained by the arrangement of silica nanoparticles, the pore in silica was just the void among particles. It indicated that the larger the particles, the lower BET surface area of the mesoporous silica derived from them. This was in keeping with the results of Kurumada [21] for similar microparticle gel systems. Besides, the BET surface area of mesoporous silica synthesized from both S/B and S methods decreased with the aging time increasing. And the reduced values tended to decrease with the ammonia concentration increasing. In the Stöber process, a certain amount of TEOS, monomers and nuclei remained in the colloidal silica sol after the reaction. Those monomers and nuclei would act as the linkage among silica nanoparticles, which caused the random arrangement of silica nanoparticles. During the aging process, the formation of silica particles and Ostwald ripening process still took place. As the aging time extended, the amount of TEOS, monomers and nuclei reduced. So the BET surface area of silica decreased with the prolonging of aging time. As depicted in Table 1, at low ammonia concentrations (0.1-0.2 mol/L), the BET surface area of the silica obtained from both the S/B and S methods decreased after the aging process. Because the amount of TEOS, monomers and nuclei in the sol was less at higher ammonia concentrations, the aging process had less effect on the BET surface area of silica. At high ammonia concentrations (0.4-0.8 mol/L), the BET surface area remained almost steady with the aging time increasing. Because, silica nanoparticles obtained from the S/B method were smaller than that of S method. It was also noticeable that the mesoporous silica obtained from the S/B method possessed a larger BET surface area than that of the S method at the same reaction condition. Furthermore, the BET surface area of mesoporous silica synthesized from the low-humidity drying method was higher than that of the high-humidity drying method. It meant that the self-assembly of the silica nanoparticles was affected by the humidity in the drying process. For the colloidal silica sol dried at the high humidity, it took a long time for evaporation. Therefore, the uniform packing of particles resulted. The amount of TEOS, monomers and nuclei in the solution was reduced due to the long time drying process. As a result, the high-humidity drying process led to the small BET surface area of silica.

Table 1. BET surface areas of the mesoporous silica as a function of aging time of the colloidal silica sol

Sample	0 h (m^2/g)	24 h (m^2/g)	48 h (m^2/g)	72 h (m^2/g)
S/B-0.1M-5%RH	393	354	302	
S/B-0.1M-90%RH		307	285	258
S/B-0.2M-5%RH	333	309	291	
S/B-0.2M-90%RH		284	255	213
S/B-0.4M-5%RH	104	103	103	
S/B-0.4M-90%RH		102	99	100
S/B-0.8M-5%RH	51	45	44	
S/B-0.8M-90%RH		51	45	43
S -0.1M-5%RH	355	278	269	
S-0.1M-90%RH		250	232	220
S-0.2M-5%RH	171	146	136	
S-0.2M-90%RH		134	130	129
S-0.4M-5%RH	95	86	68	
S-0.4M-90%RH		69	61	55
S-0.8M-5%RH	40	39	33	
S-0.8M-90%RH		31	35	31

3. The Effect of Aging Process on the Pore Structure of Mesoporous Silica Synthesized from the Self-assembly of Silica Nanoparticles

Fig. 4 presents nitrogen adsorption-desorption isotherms of the mesoporous silica synthesized at different ammonia concentrations.

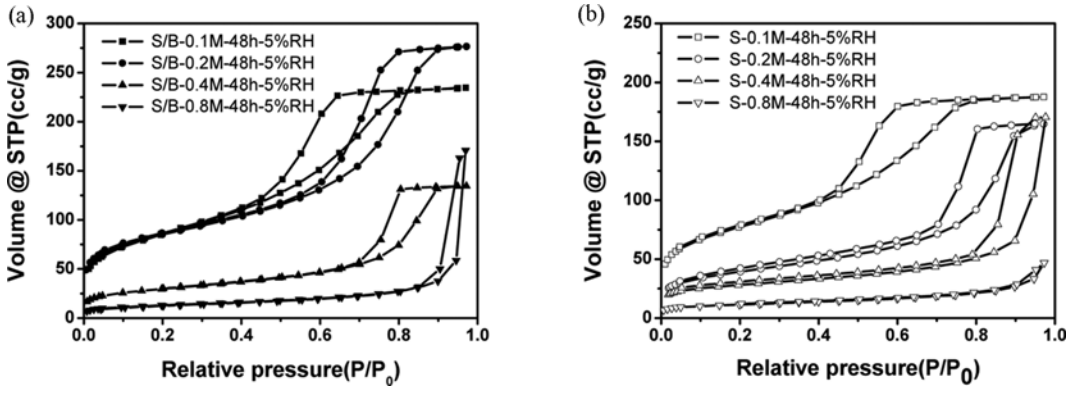

Fig. 4. Nitrogen adsorption-desorption isotherms of silica: (a) S/B-M-48h-5%RH; (b) S-M-48h-5%RH.

The isotherms of mesoporous silica obtained at the ammonia concentration of 0.1-0.4 mol/L exhibited the typical IV pattern with a H2 hysteresis loop as defined by IUPAC [22]. Furthermore, the isotherm shows a clear H2 hysteresis loop, which is characterized by a smoothly increasing adsorption branch and a steep desorption branch. Commonly, type H2 hysteresis is attributed to ink bot-

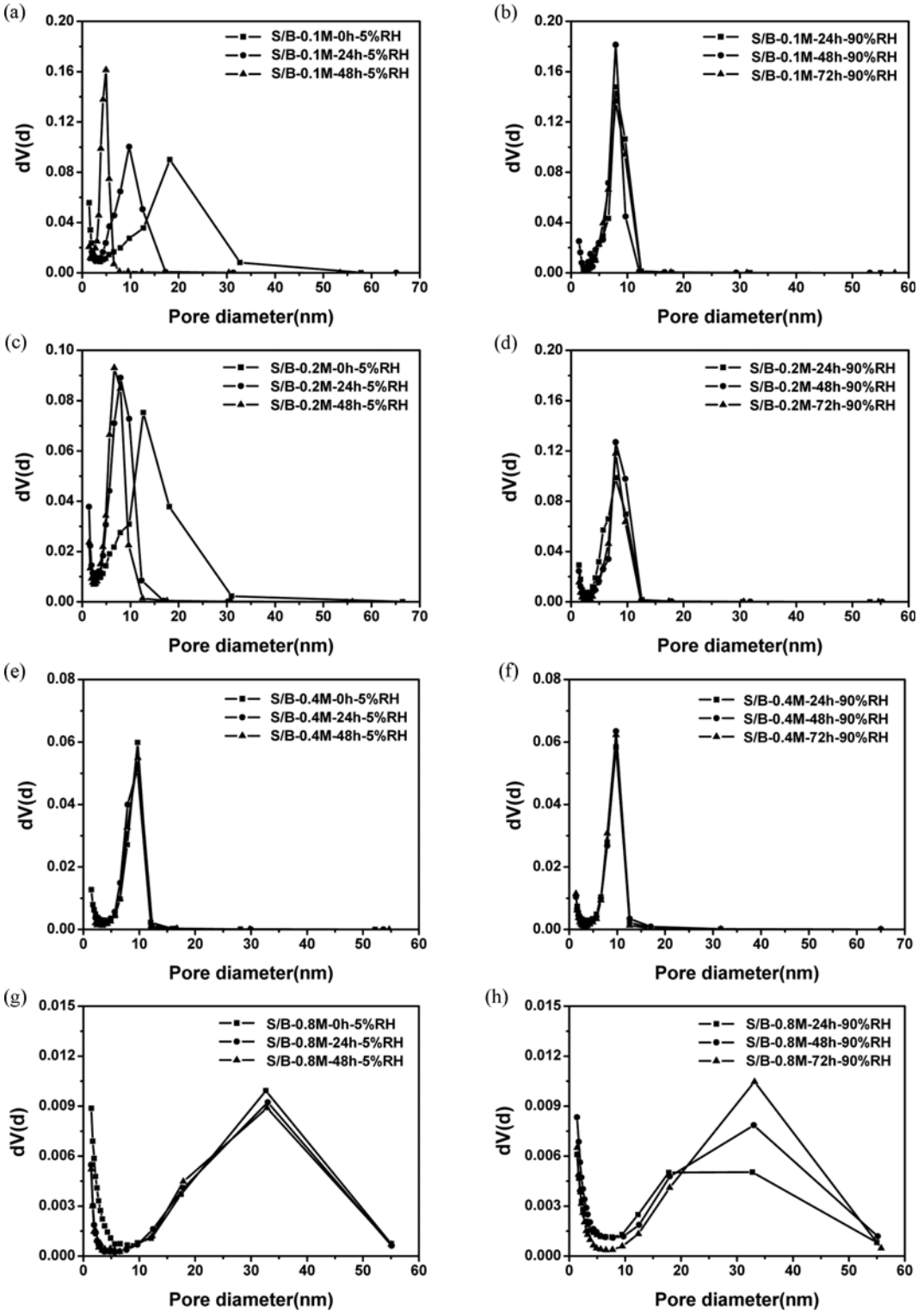

Fig. 5. The effect of aging time, ammonia concentration and drying method on the pore size of mesoporous silica synthesized from the S/B method. (a) C_{NH4OH}=0.1 mol/L, RH=5%; (b) C_{NH4OH}=0.1 mol/L, RH=90%; (c) C_{NH4OH}=0.2 mol/L, RH=5%; (d) C_{NH4OH}=0.2 mol/L, RH=90%; (e) C_{NH4OH}=0.4 mol/L, RH=5%; (f) C_{NH4OH}=0.4 mol/L, RH=90%; (g) C_{NH4OH}=0.8 mol/L, RH=5%; (h) C_{NH4OH}=0.8 mol/L, RH=90%.

tle shaped pores, having a narrow entrance and a wider body. In our case, ink bottle-shaped pores or voids were generated by the arrangement of silica nanoparticles [23]. When the ammonia concentration was 0.8 mol/L, the type of isotherm changed from type IV to type II, which was in a good agreement with the results of Watanable et al. [11] and Wang et al. [24]. It was also depicted in Fig. 4 that the pore volume of mesoporous silica synthesized from both S/B and S methods decreased with the ammonia concentration increasing.

The pore sizes of mesoporous silica synthesized from the S/B method are listed in Fig. 5, which shows that the pore size increased with the ammonia concentration increasing. As discussed previously, the pores in silica were obtained by the arrangement of nanoparticles. Thus, the large silica nanoparticles obtained at high ammonia concentrations resulted in large voids among nanoparticles. For the silica obtained from the colloidal sol (S/B-24h-5%RH), the pore diameter at the ammonia concentration of 0.1 mol/L, 0.2 mol/L, 0.4 mol/L and 0.8 mol/L was 4.9 nm, 7.9 nm, 9.7 nm and 33 nm, respectively. In addition, the pore size distribution of mesoporous silica at various ammonia concentrations was different. Among the four samples (S/B-0.1M-72h-90%RH, S/B-0.2M-72h-90%RH, S/B-0.4M-72h-90%RH and S/B-0.8M-72h-90%RH), S/B-0.4M-72h-90%RH had the narrowest pore size distribution, and S/B-0.8M-72h-90%RH possessed the widest pore size distribution. The different pore size distribution resulted from the various packing qualities of silica nanoparticles. The uniform particles led to the narrow pore size distribution. This observation is in consistent with results from other studies on the self-assembly of nanoparticles [25,26].

The pore size of mesoporous silica could also be controlled through the aging treatment of the colloidal silica sol. Fig. 5 also exhibits the various pore properties of mesoporous silica after aging treatment of the corresponding colloidal silica sol at 25 °C for 0, 24 and 48 hours, respectively. After the 48 hours' aging treatment of colloidal silica sol, the pore size of S/B-0.1M-5%RH in Fig. 5(a) reduced from 18 nm to 4.9 nm, and the pore size of S/B-0.2M-5%RH in Fig. 5(c) also decreased from 12.7 nm to 6.6 nm. In addition, both of them had narrow pore size distributions after the aging treatment. As shown in Fig. 5(b), 5(d), 5(f) and 5(h), the aging treatment had limited impact on the pore size of mesoporous silica obtained from the high-humidity drying method. Compared with the aging process, the drying condition possessed a stronger effect on the pore structure of mesoporous silica. Furthermore, Fig. 5(e), 5(f), 5(g) and 5(h) show that the pore structure of mesoporous silica was seldom affected by the aging treatment at the ammonia concentration from 0.4 mol/L to 0.8 mol/L. Above all, the aging treatment resulted in the silica with decreased pore size and narrow pore size distribution.

The pore size of the mesoporous silica could be controlled by drying the colloidal silica sol at different humidity. Comparing S/B-0.1M-0h-5%RH and S/B-0.1M-24h-90%RH, S/B-0.2M-0h-5%RH and S/B-0.2M-24h-90%RH clearly shows that the pore size of silica was reduced at the high humidity. Besides, the pore (2-5 nm) of silica was also reduced at the high humidity. When the colloidal silica sol was dried in the high-humidity condition, it took a long time to evaporate the solvent. Then the slow arrangement of silica nanoparticles resulted in the good packing quality. First, the long-time Ostwald ripening at the high-humidity condition led to the decreased amount of small particles. Second, the hydrogen bond of silica sub-particles at the high water concentration was strong [9]. And sub-particles at the high water concentration agglomerated with each other or grew into large particles [9]. Therefore, the amount of small pores (2-5 nm) in the mesoporous silica decreased. As can be seen in Fig. 5(e), 5(f), 5(g) and 5(h), the drying humidity almost had no influence on the pore structure of mesoporous silica obtained at the ammonia concentration from 0.4 mol/L to 0.8 mol/L. Because the amount of TEOS, monomers and nuclei in the colloidal sol at the high ammonia concentration was small.

Fig. 5 demonstrates that the aging treatment and drying method seldom affected the pore structure of silica at the ammonia concentration of 0.4-0.8 mol/L. The concentration of monomers and sub-particles was low at the high ammonia concentration. In the Stöber process, those monomers and sub-particles could act as the linkage between particles, form new particles or lead to the regrowth of nanoparticles [27], which affects the pore structure of mesoporous silica. Owing to the low condensation rate of Si-OH groups among particles at the high pH, silica nanoparticles could rearrange freely even at the final stage of evaporation under the influence of capillary force to form tightly packed nanostructure [24]. On the basis of the above discussion, the colloidal silica sol at the high ammonia concentration is seldom influenced by the aging treatment and drying process.

The pore size of mesoporous silica synthesized from the S method is listed in Fig. 6, which shows the same trend as that of the S/B method. The pore size increased with the ammonia concentration rising. For the colloidal silica sol synthesized at the ammonia concentration of 0.8 mol/L, the pore size was in a wide range due to the wide size distribution of silica particles.

Both the results of Fig. 5 and Fig. 6 indicate that the pore size and pore distribution of mesoporous silica were in accordance with the size and distribution of silica nanoparticles. The pore size of silica obtained from the S/B method was almost the same as that of the S method at the ammonia concentration of 0.1 mol/L. The pore size of silica obtained from the S method was larger than that of the S/B method at the ammonia concentration of 0.2-0.4 mol/L. All those results agreed with the results of DLS. It is easy to understand that the pore was the void of packing silica nanoparticles. A narrow pore distribution was achieved by synthesizing silica nanoparticles with a narrow size distribution, aging for a certain period and then drying at the high-humidity condition.

CONCLUSIONS

Two economical methods (semi-batch and semi-batch/batch) were demonstrated to synthesize silica nanoparticles with different sizes (ranging from 10 nm to 104 nm) and size distributions using ammonia as the base catalyst. Then the amorphous silica with different surface areas (ranging from 30 m^2/g to 400 m^2/g) and pores (ranging from 3 nm to 33 nm) were obtained by various aging treatments and drying methods of the synthesized colloidal silica sol. The aging treatment resulted in uniform pore distribution and decreased BET surface area of silica. And the high-humidity drying method resulted in the uniform pore distribution and decreased

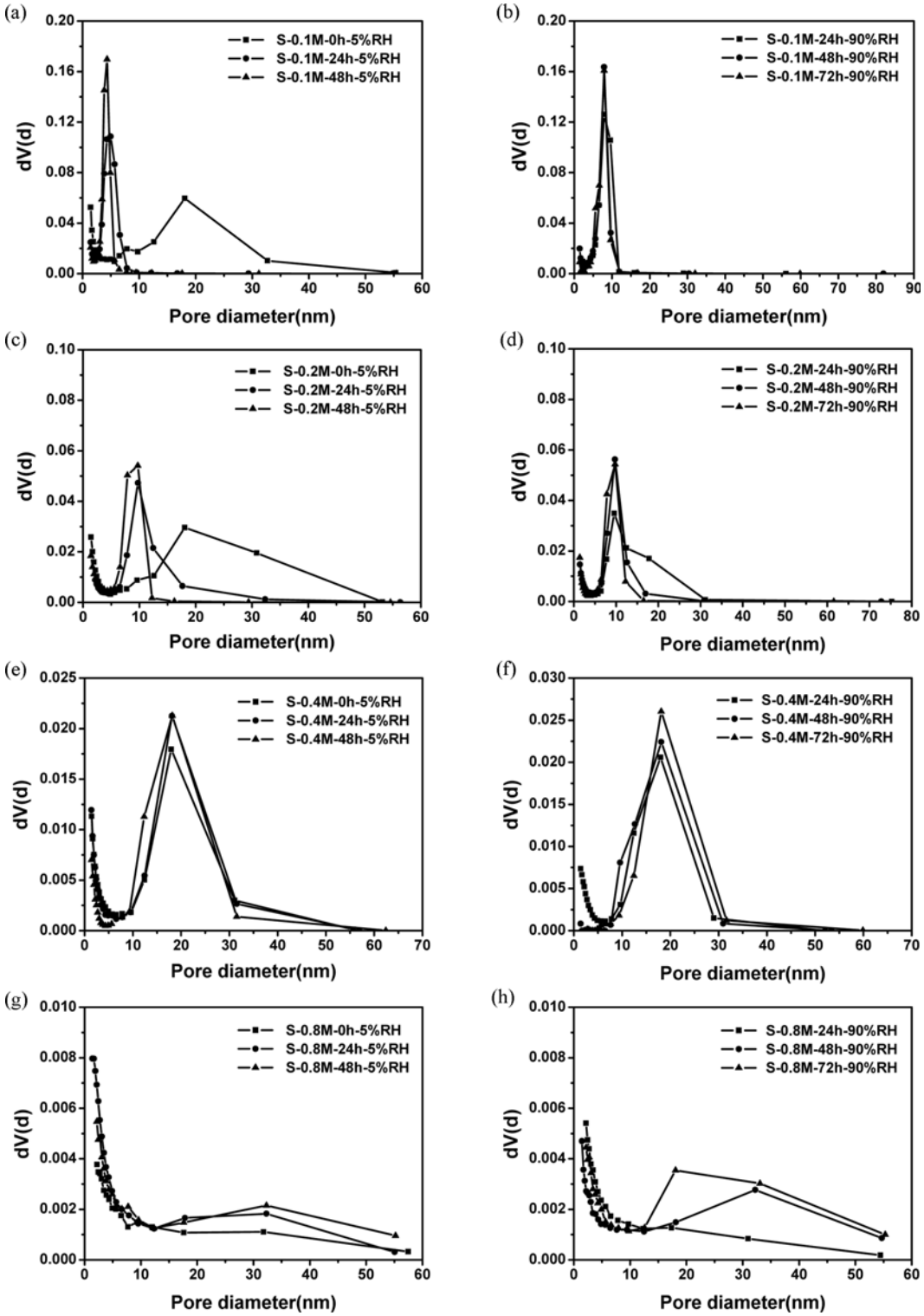

Fig. 6. The effect of aging, ammonia concentration and drying method on the pore structure of mesoporous silica synthesized from the S method. (a) C_{NH4OH}=0.1 mol/L, RH=5%; (b) C_{NH4OH}=0.1 mol/L, RH=90%; (c) C_{NH4OH}=0.2 mol/L, RH=5%; (d) C_{NH4OH}=0.2 mol/L, RH=90%; (e) C_{NH4OH}=0.4 mol/L, RH=5%; (f) C_{NH4OH}=0.4 mol/L, RH=90%; (g) C_{NH4OH}=0.8 mol/L, RH=5%; (h) C_{NH4OH}=0.8 mol/L, RH=90%.

small pore of mesoporous silica. Besides, the pore diameter and pore distribution of mesoporous silica were directly related to the size and distribution of silica nanoparticles in the colloidal sol. To obtain the monodispersed pore distribution of mesoporous silica, the aging treatment of colloidal sol and high-humidity drying method were all demonstrated facile routes. Furthermore, this study offered

a new insight for the synthesis of other mesoporous materials with uniform pore distributions.

REFERENCES

1. L. W. Hrubesh, P. R. Coronado and J. H. Satcher Jr., *J. Non-Cryst. Solids*, **285**, 328 (2001).
2. C. A. Morris, M. L. Anderson, R. M. Stroud, C. I. Merzbacher and D. R. Rolison, *Science*, **284**, 622 (1999).
3. I. Smirnova, S. Suttiruengwong and W. Arlt, *J. Non-Cryst. Solids*, **350**, 54 (2004).
4. W. Stöber, A. Fink and E. Bohn, *J. Colloid Interface Sci.*, **26**, 62 (1968).
5. Y. Huang and J. E. Pemberton, *Colloids Surf., A*, **377**, 76 (2011).
6. Z. B. Lei, Y. Xiao, L. Q. Dang, M. Lu and W. S. You, *Micropor. Mesopor. Mater.*, **96**, 127 (2006).
7. R. Lindberg, J. Sjöblom and G. Sundholm, *Colloids Surf., A*, **99**, 79 (1995).
8. H. Scott Fogler, *Elements of Chemical Reaction Engineering*, Prentice-Hall of India (2004).
9. K. D. Kim and H. T. Kim, *J. Sol-Gel Sci. Technol.*, 25, **183** (2002).
10. K. D. Hartlen, A. P. T. Athanasopoulos and V. Kitaev, *Langmuir*, **24**, 1714 (2008).
11. R. Watanabe, T. Yokoi, E. Kobayashi, Y. Otsuka, A. Shimojima, T. Okubo and T. Tatsumi, *J. Colloid Interface Sci.*, **360**, 1 (2011).
12. J. W. Tang, X. F. Zhou, D. Y. Zhao, G. Q. Lu, J. Zou and C. Z. Yu, *J. Am. Chem. Soc.*, **129**, 9044 (2007).
13. Y. Kuroda, Y. Yamauchi and K. Kuroda, *Chem. Commun.*, **46**, 1827 (2010).
14. S. A. Johnson, P. J. Ollivier and T. E. Mallouk, *Science*, **283**, 963 (1999).
15. K. Nozawa, H. Gailhanou, L. Raison, P. Panizza, H. Ushiki, E. Sellier, J. P. Delville and M. H. Delville, *Langmuir*, **21**, 1516 (2005).
16. G. H. Bogush and C. F. Zukoski, *J. Colloid Interface Sci.*, **142**, 1 (1991).
17. V. K. LaMer and R. H. Dinegar, *J. Am. Chem. Soc.*, **72**, 4847 (1950).
18. D. L. Green, J. S. Lin, Y. F. Lam, M. Z. C. Hu, D. W. Schaefer and M. T. Harris, *J. Colloid Interface Sci.*, **266**, 346 (2003).
19. T. Matsoukas and E. Gulari, *J. Colloid Interface Sci.*, **124**, 252 (1988).
20. C. J. Brinker and G. W. Scherer, *Sol-Gel Science: The Physics and Chemistry of Sol-Gel Processing*, Academic Press, Boston (1990).
21. K. I. Kurumada, H. Nakabayashi, T. Murataki and M. Tanigaki, *Colloids Surf., A*, **139**, 163 (1998).
22. K. S. W. Sing, D. H. Everett, R. A. W. Haul, L. Moscou, R. A. Pierotti, J. Rouquerol and T. Siemieniewska, *Pure Appl. Chem.*, **57**, 603 (1985).
23. S. Lee, I. S. Cho, J. H. Lee, D. H. Kim, D. W. Kim, J. Y. Kim, H. Shin, J. K. Lee, H. S. Jung, N. G. Park, K. Kim, M. J. Ko and K. S. Hong, *Chem. Mater.*, **22**, 1958 (2010).
24. J. Z. Wang, A. Sugawara-Narutaki, M. Fukao, T. Yokoi, A. Shimojima and T. Okubo, *ACS Appl. Mater. Interfaces*, **3**, 1538 (2011).
25. C. Wang, Y. H. Zhang, L. Dong, L. M. Fu, Y. B. Bai, T. J. Li, J. G. Xu and Y. Wei, *Chem. Mater.*, **12**, 3662 (2000).
26. R. Micheletto, H. Fukuda and M. Ohtsu, *Langmuir*, **11**, 3333 (1995).
27. Y. Huang and J. E. Pemberton, *Colloids Surf., A*, **360**, 175 (2010).